Application note | 003385

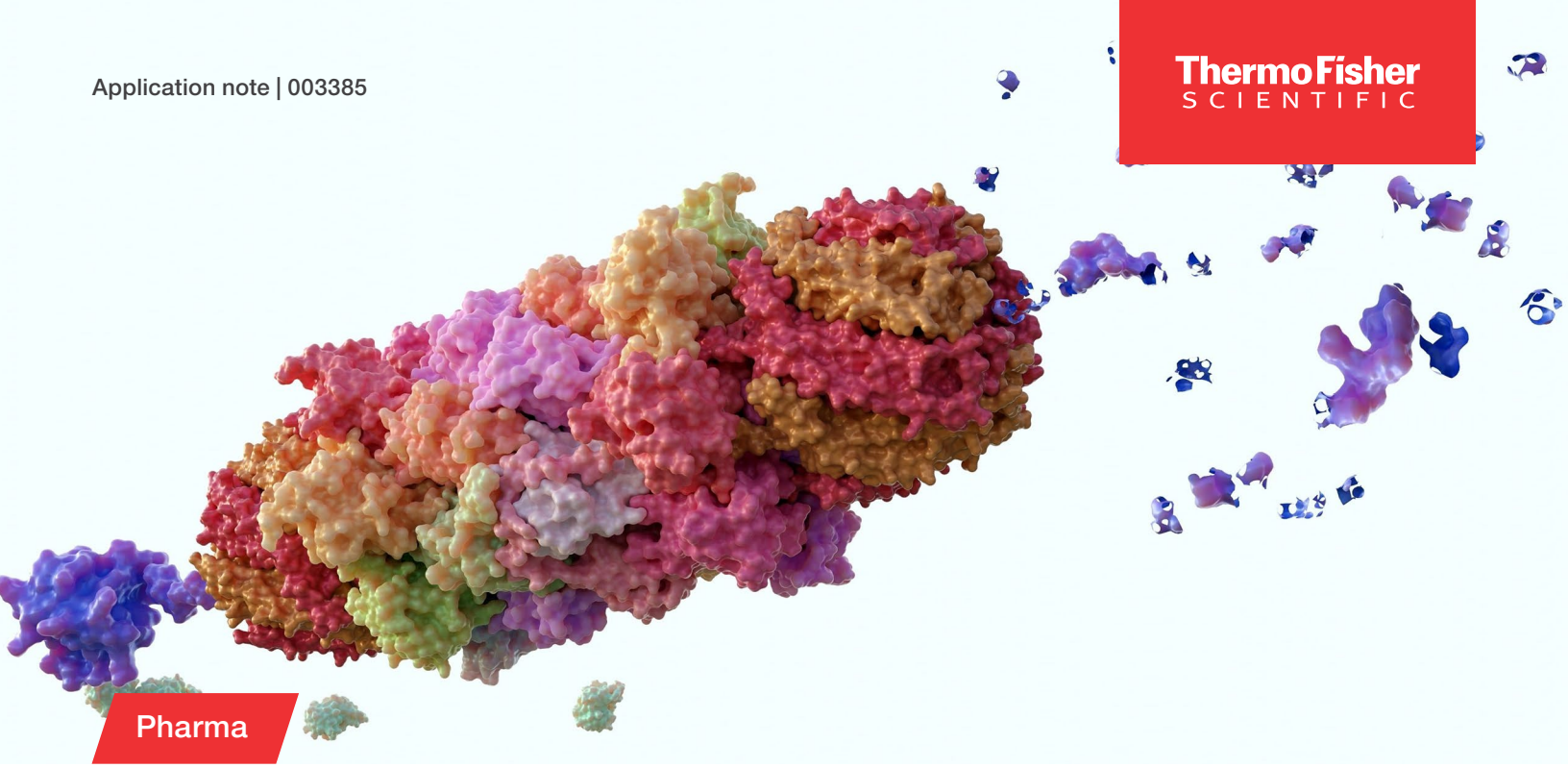

Pharma

Confident transformation site localization of PROTAC drug metabolites facilitated by multi-stage fragmentation LC-MS

Authors

Sven Hackbusch[1], Min Du[2]

[1]Thermo Fisher Scientific, San Jose, CA, USA

[2]Thermo Fisher Scientific, Lexington, MA, USA

Keywords

PROTAC, Metabolite identification (MetID), structure elucidation, Orbitrap Ascend BioPharma Tribrid mass spectrometer, high-resolution accurate mass (HRAM), MS^n, Vanquish Horizon UHPLC system, Compound Discoverer software, biotransformation

Application benefits

- Confident detection and structure elucidation of low abundant PROTAC drug metabolites using high-quality MS^2 and MS^3 data from the Thermo Scientific™ Orbitrap™ Ascend Biopharma Tribrid™ mass spectrometer
- Automated detection of metabolites and fragment structure assignment to facilitate transformation site localization within the Thermo Scientific™ Compound Discoverer™ software

Goal

Demonstrate the characterization of drug metabolites from in vitro incubations of bifunctional PROTAC model drug compounds, and the utility of intelligently acquired MS^n fragmentation data for transformation site localization and soft-spot analysis.

Introduction

The study of a drug's metabolism is an integral part of drug discovery and development, from improving drug exposure to flagging potential toxicity from its metabolites. The identification of drug metabolites routinely relies on LC-MS experiments, with fragmentation data enabling their structure elucidation. In recent years, hetero-bifunctional small molecule drugs, acting on a given protein of interest (POI) through

recruitment of inherent protein degradation pathways rather than inhibition, have gained significant interest as new modalities, with multiple-such proteolysis targeting chimera (PROTAC™)-drug candidates being investigated in clinical trials.[1] However, due to PROTAC's unique properties, the identification of their metabolites can be challenging.[2]

Here, we present a case study for metabolite profiling of model PROTAC compounds and the utility of multi-stage fragmentation (MS^n) for the elucidation of transformation sites, based on analysis of the representative compounds shown in Figure 1A.

Experimental

Chemicals and consumables

- MZ1 (MedChemExpress, CAS 1797406-69-9, P/N HY-107425)
- dBET1 (MedChemExpress, CAS 1799711-21-9, P/N HY-101838)
- Thermo Scientific™ Pierce™ Dimethylsulfoxide (DMSO), LC-MS grade (P/N 85190)
- Pooled human liver S9 fraction, mixed gender (XenoTech) (P/N H0620.S9)
- Thermo Scientific™ Phosphate, 0.5 M buffer solution, pH 7.4 (P/N J60785.AP)
- Thermo Scientific™ NADPH tetrasodium salt hydrate (P/N 328742500)
- Fisher Chemical™ Formic acid, 99.0+%, Optima™ LC/MS grade (P/N A117-50)
- Thermo Scientific™ Water, UHPLC grade, 1 L (P/N W8-1)
- Thermo Scientific™ Acetonitrile, UHPLC grade, 1 L (P/N A956-1)
- Thermo Scientific™ SureSTART™ Screw Glass Vial, 2 mL, Level 3 (P/N 6PSV9-1PSS)
- Thermo Scientific™ SureSTART™ 9 mm Screw Caps, Level 3 (P/N 6PSC9TST)

Sample preparation

The test articles (MZ1, dBET1) were dissolved in DMSO (1 mM stock concentration), respectively, and incubated at a concentration of 5 µM with human liver S9 fraction (1 mg/mL) in 100 mM phosphate buffer (held at 37 °C, final DMSO concentration 0.5%). The reactions were initiated with the addition of NADPH (1 mM), before terminating the enzymatic reactions after 0 or 4 hours with the addition of 1 equivalent of ice-cold acetonitrile. All metabolism sample and matrix blank (DMSO vehicle) incubations were then centrifuged at 5,000 rpm for 5 minutes before transferring the supernatant into glass autosampler vials for analysis using LC-MS.

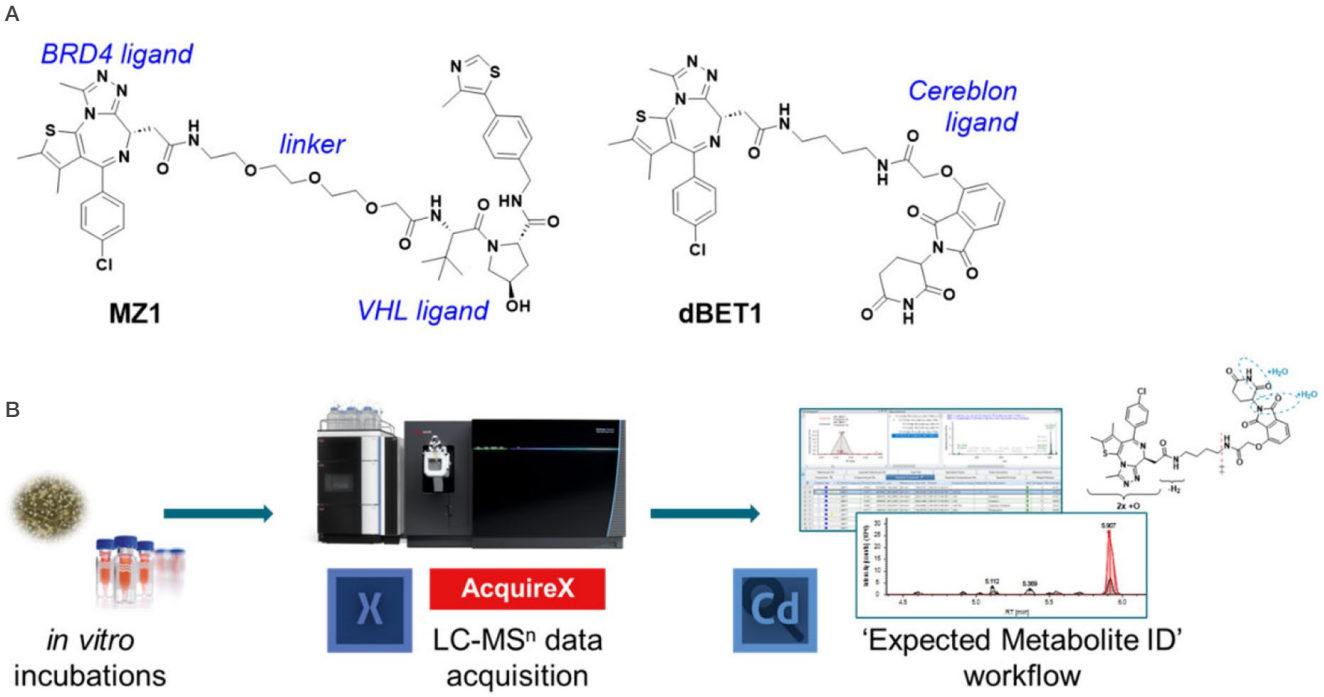

Figure 1. (A) Structures of the model PROTAC compounds MZ1 and dBET1 with shared BRD4 ligand substructure; (B) overview of Metabolite ID application steps from *in vitro* incubations of the test articles, LC-MS data acquisition using intelligent MS^n data acquisition, to data processing facilitated by the "Expected Metabolite ID" workflow in the Compound Discoverer software

Instrumentation

Liquid chromatography

Thermo Scientific™ Vanquish™ Horizon system consisting of:

- Vanquish System Base (P/N VH-S01-A-02)
- Vanquish Binary Pump H (P/N VH-P10-A-01)
- Sampler HT (P/N VH-A10-A-02)
- Vanquish Column Compartment H (P/N VH-C10-A-02)
- Vanquish Diode Array Detector FG (P/N VF-D11-A-01)
- Standard flow cell, path length 10 mm (13 µL, SST) (P/N 6083.0510)
- MS Connection Kit Vanquish (P/N 6720.0405)

Table 1. Chromatographic conditions

Parameter	Value
Column	Thermo Scientific™ Accucore™ C18 (2.1 × 100 mm, 2.6 µm)
Mobile phases	A: 0.1% formic acid in water B: 0.1% formic acid in acetonitrile
Gradient	Time (min) % A % B 0 95 5 1 95 5 10 5 95 15 5 95 15.1 95 5 20 95 5
Flow rate	0.4 mL/min
Column temperature	45 °C
Autosampler temperature	4 °C
Autosampler wash solvent	50:50 water:acetonitrile
Injection volume	1 µL
Diode array detector settings	254 nm, 2 Hz

Mass spectrometry

Mass spectrometry data was acquired using the Orbitrap Ascend Biopharma Tribrid mass spectrometer (P/N B51003849) equipped with a Thermo Scientific™ OptaMax™ NG heated electrospray ionization (H-ESI) ion source and operated with the Orbitrap Tribrid Series 4.1 SP1 instrument control software. Untargeted drug metabolite profiling experiments on the test article samples were carried out using a single polarity TopSpeed data-dependent MS^n ($ddMS^n$) experiment. A Thermo Scientific™ EASY-IC™ internal calibration ion source was employed for all data acquisitions to ensure high mass accuracy throughout the data acquisition. The MS source conditions and important MS experiment parameters are detailed in Tables 2 and 3.

Table 2. MS H-ESI source conditions overview

Parameter	Value
Spray voltage	+3,250 V
Sprayer position	1.5, M/H, center
Vaporizer temperature	325 °C
Ion transfer tube temperature	300 °C
Sheath gas	40 a.u.
Aux gas	10 a.u.
Sweep gas	1 a.u.

Table 3. MS method parameter overview

Parameter	Value
Acquisition type	Full Scan – data-dependent $MS^{2/3}$
Cycletime (TopSpeed)	0.8 s
MS^1 resolution	60,000 @ *m/z* 200
MS^1 mass range	*m/z* 150–1,500
RF level, %	40
Lock mass correction	Scan-to-Scan Easy-IC
MS^2 intensity threshold	1e5
Dynamic exclusion	4 s
MS^2 exclusion list	Populated using AcquireX Background Exclusion workflow and matrix blank sample
MS^n decision tree	<500 Da: MS^2-HCD >500 Da: MS^2-CID + MS^3-CID / MS^2-HCD MS^3 criteria: >350 Da and >15% (up to 3) (see Figure 2)
MS^2-CID collision energy	30%
MS^2-HCD collision energy (normalized, stepped)	15, 30, 45%
MS^2 maximum injection time	50 ms
MS^3 maximum injection time	100 ms

Software

The Thermo Scientific™ Xcalibur 4.7 software was used for data acquisition, employing the Thermo Scientific™ AcquireX™ Background Exclusion workflow for intelligent fragmentation data acquisition. Data processing was carried out using the Expected Metabolite Identification workflow in Compound Discoverer 3.3 SP3 software.

Results and discussion

MS^n data acquisition approach

Fragmentation data is essential to go beyond the detection of the transformation products formed from the parent drug and enable the elucidation of transformation sites. Beyond conventional HCD-MS^2 fragmentation, the Orbitrap Ascend Biopharma Tribrid MS enables the acquisition of multi-stage (MS^n) fragmentation data using its dual-pressure linear ion trap. Using CID fragmentation (performed in the ion trap, and leading to step-wise fragmentation), MS^n spectra can be particularly helpful to distinguish isomeric metabolites and cases where ambiguity exists in the assignment of fragment structures. To increase the utility of MS^n data collected in a data-dependent fashion, the Orbitrap Tribrid MS series allows the user to set up method decision trees that change the spectra acquired for each precursor on-the-fly. Additionally, the AcquireX intelligent data acquisition Background Exclusion workflow was used to generate a comprehensive exclusion list of background ions (*m/z*, RT, intensity threshold) from the injection of the matrix blank sample, focusing MS^n data acquisition on only sample-relevant compounds, which has been shown to increase the fragmentation coverage in metabolite ID experiments, thereby reducing the need for data reacquisition with targeted MS^n methods.[3]

The analysis of the metabolism of MZ1 and dBET1 from incubations with human liver S9 fractions was carried out using a Full Scan data-dependent MS^n acquisition method that followed the decision tree structure detailed in Table 3 and Figure 2. Data acquisition was thus adapted on-the-fly depending on the precursor masses and obtained fragmentation spectra at a given moment to maximize the relevant data and enable structure elucidation. Within a cycle time of 0.8 s (ensuring sufficient sampling of the Full Scan across eluting peaks), the instrument either collected just MS^2-HCD spectra for those precursors below 500 Da that passed the Intensity, isotope exclusion, targeted mass exclusion, and dynamic exclusion filters, while collecting MS^2-CID spectra and up to 3 scans of MS^3-CID and MS^2-HCD spectra for precursors above 500 Da. Figure 3 shows an example of the resulting data that was collected by the instrument based on the parent MZ1 and one of its metabolites detected in the 4 hr timepoint.

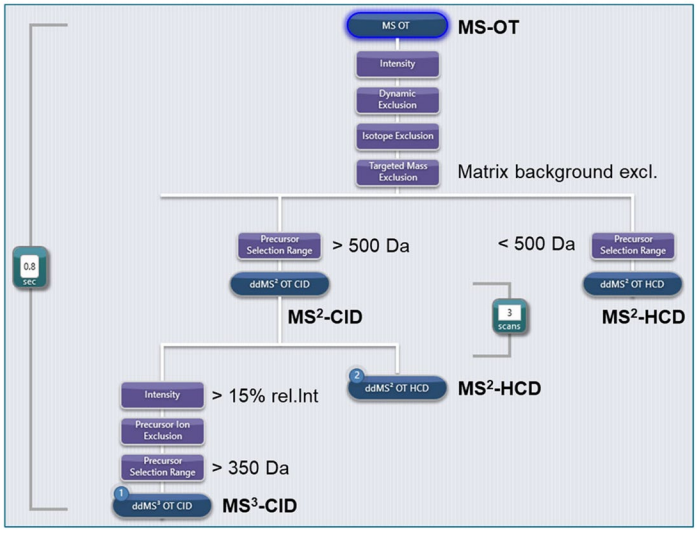

Figure 2. Experiment decision tree used to acquire MS^n data in versatile fashion, with MS^3 data acquired only on precursors exceeding 500 Da to increase efficiency

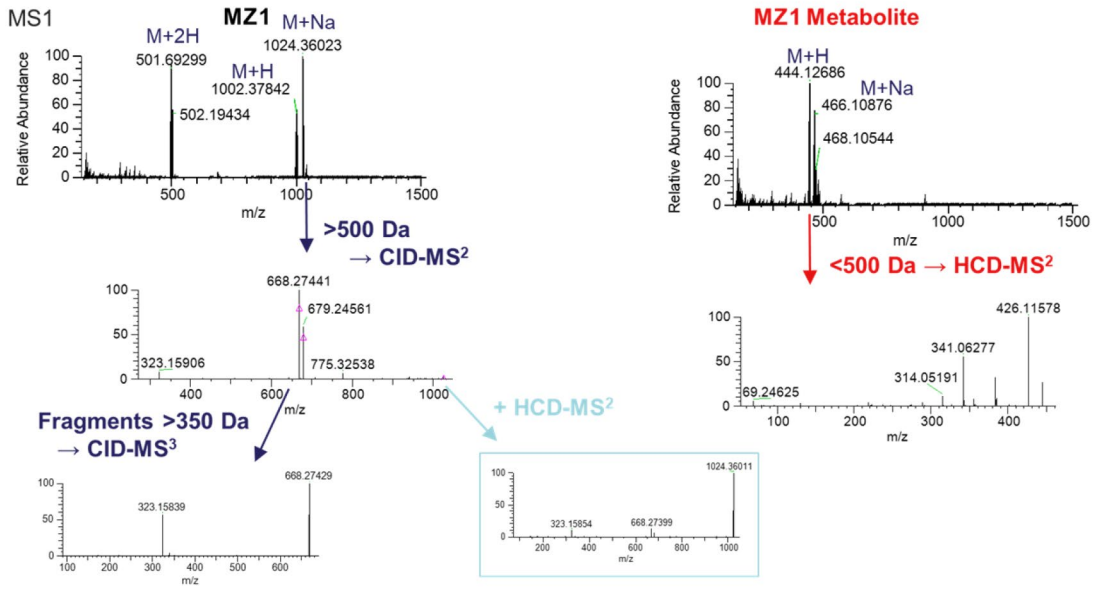

Figure 3. MS^1 spectra of MZ1 and one of its metabolites (M10), as well as the fragmentation data acquired based on the respective precursor *m/z* and observed MS^2 fragments using the versatile MS^n method decision tree detailed in Figure 2

Data overview and Compound Discoverer software processing

From the overlay of the two different timepoints of the incubation with MZ1, the reduction of the parent peak at 6.36 min and appearance of several more polar metabolites was readily apparent from the total ion chromatograms, as shown in Figure 4. The high-resolution accurate mass (HRAM) data from the Orbitrap Ascend Biopharma Tribrid MS allowed the confident detection of these peaks and assignment of elemental compositions. Similarly, the metabolite peaks observed for dBET1 were also more polar than the parent compound (data not shown).

High-quality HRAM full scan and ddMS^2 data enable the detection and identification of drug metabolites; however, due to the sample complexity and sensitivity, an effective data mining tool is essential for confident metabolite identification. In this study, the data processing was carried out using the Compound Discoverer software, which uses a fully customizable node-based processing workflow to process HRAM full scan MS, associated MS^n data, and fine isotope patterns for structure identification and database searching to enable small molecule identification. Specific to the identification of drug metabolites, a targeted peak detection approach was utilized to detect "Expected Compounds" and facilitate their identification with the fragment ion search (FISh) scoring node, as outlined in Figure 5.

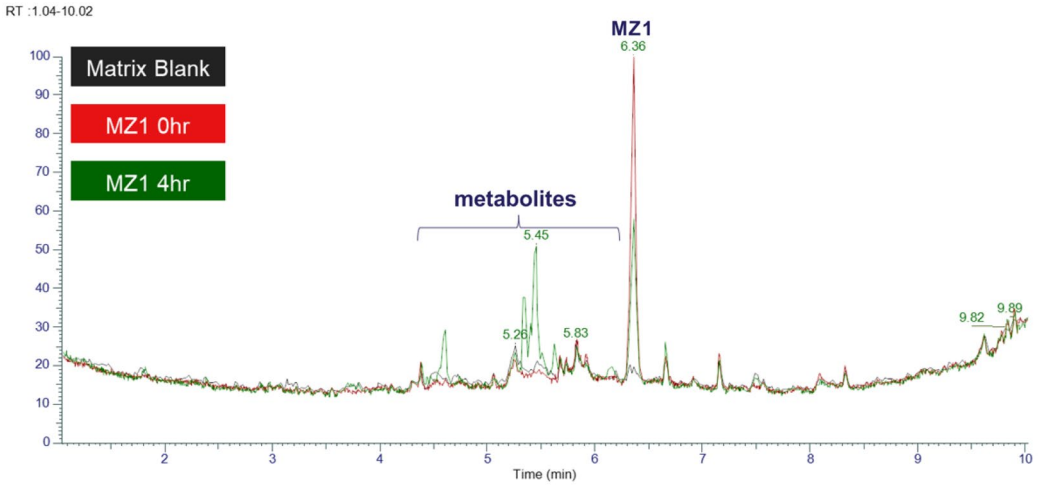

Figure 4. Total ion chromatogram overlays of the 0 hr and 4 hr timepoints for MZ1 and the matrix blank, showing the decrease in parent compound peak area and appearance of multiple metabolite peaks in the 4 hr sample

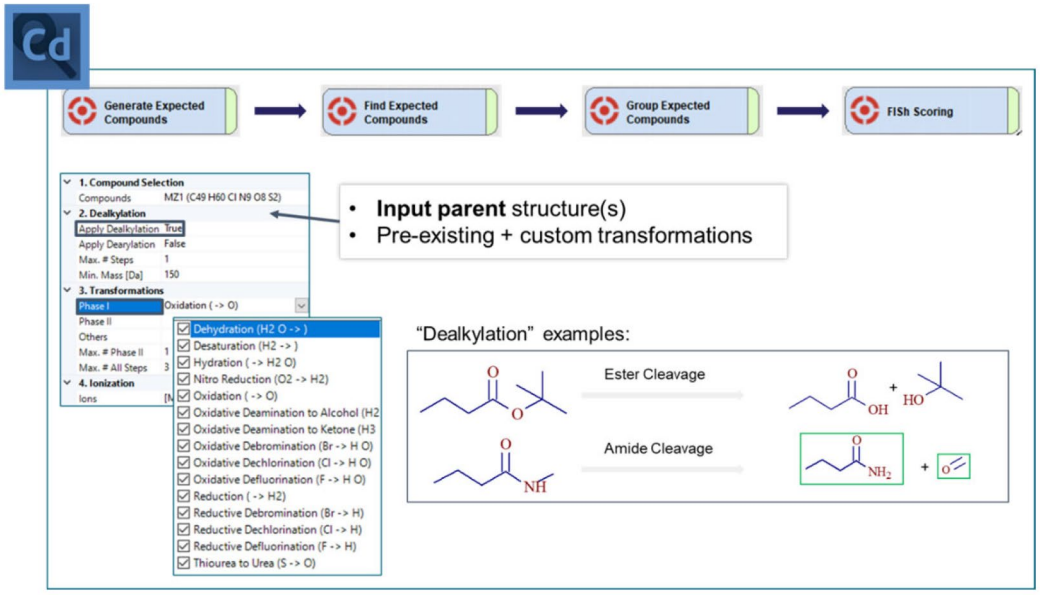

Figure 5. Outline of the targeted detection approach ("Expected Compounds") used by the Compound Discoverer software to find metabolites based on a list of transformations generated based on intelligent dealkylation predictions and expected metabolic transformations, followed by automatic annotation of matched and transformation-shifted fragments, as determined by the fragment ion search (FISh) algorithm in the FISh scoring step

For MZ1 and dBET1, a total of 24 and 12 metabolites could be detected and annotated using this approach, respectively. In the case of MZ1, the most abundant metabolites were the result of linker cleavages, as highlighted for M14 (MW 532.1778 @ 5.45 min) in Figure 6. In addition to the accurate mass measurement of multiple adducts, the software used the isotopic peak patterns to verify their elemental composition and the experimental fragmentation patterns annotated with *in silico* predicted fragments using the FISh scoring node to increasing confidence in the structure assignment during data review.

Summary of metabolism of the PROTAC test articles

The top five most abundant metabolites detected in the *in vitro* metabolism samples of MZ1 and dBET1 are summarized in Figures 7 and 8, respectively. As can be seen from the transformation sites highlighted on their structures, the linker contributed significantly to the metabolism of MZ1, while dBET1 was primarily metabolized by oxidation and hydrolytic opening of the phthalate structure. A summary of all detected and annotated metabolites for both compounds is given in the Appendix.

Use of MS^n for transformation site localization

In the case of the oxidized metabolite M18 (MW 1017.3640 @ 5.63 min), the site of oxidation could be narrowed to the BRD4 ligand or linker from the MS^2-CID spectrum of the sodium adduct, which contained several oxidation-shifted fragments. Inspection of the MS^3 spectrum of the shifted fragment at *m/z* 695 allowed to pinpoint the oxidation site to the BRD4 ligand based on the oxidation-shifted fragment at *m/z* 395, as outlined in Figure 9.

In contrast, the lower abundant "+O" metabolite M23 showed drastically different fragmentation behavior, yielding a single fragment ion significant intensity at *m/z* 641, which could be annotated with a structure corresponding to the loss of the BRD4 ligand substructure, as shown in Figure 10. The corresponding MS^3 spectrum allowed localization of the oxidation to the linker portion based on fragments that were absent from the MS^2-CID spectrum and only revealed in the subsequent fragmentation event.

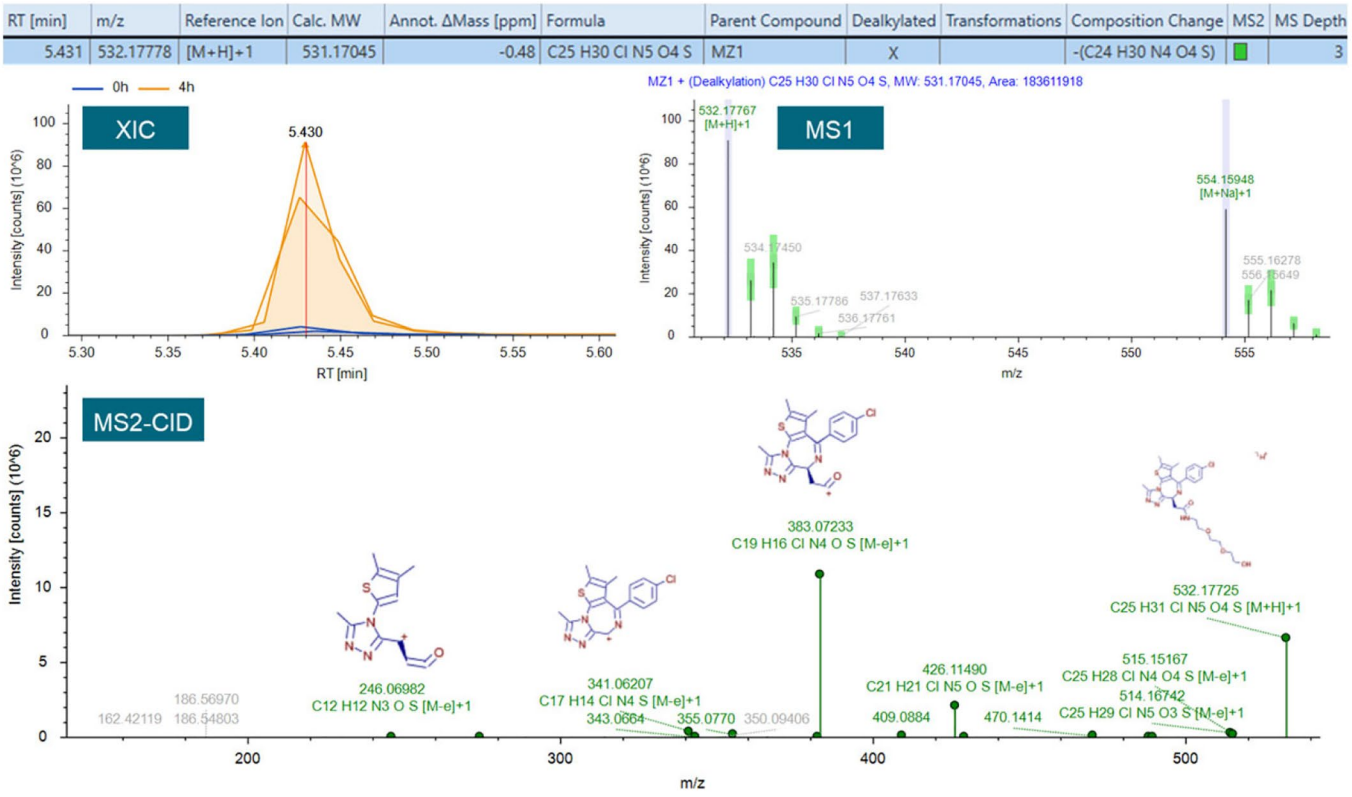

Figure 6. Overview of the MS^1 and MS^n data supporting the metabolite assignment for M14 (MW 532.1778 @ 5.45 min) resulting from a "dealkylation" linker cleavage, with fragment ions matching the *in silico* predicted fragments of the metabolite automatically highlighted in the Compound Discoverer software

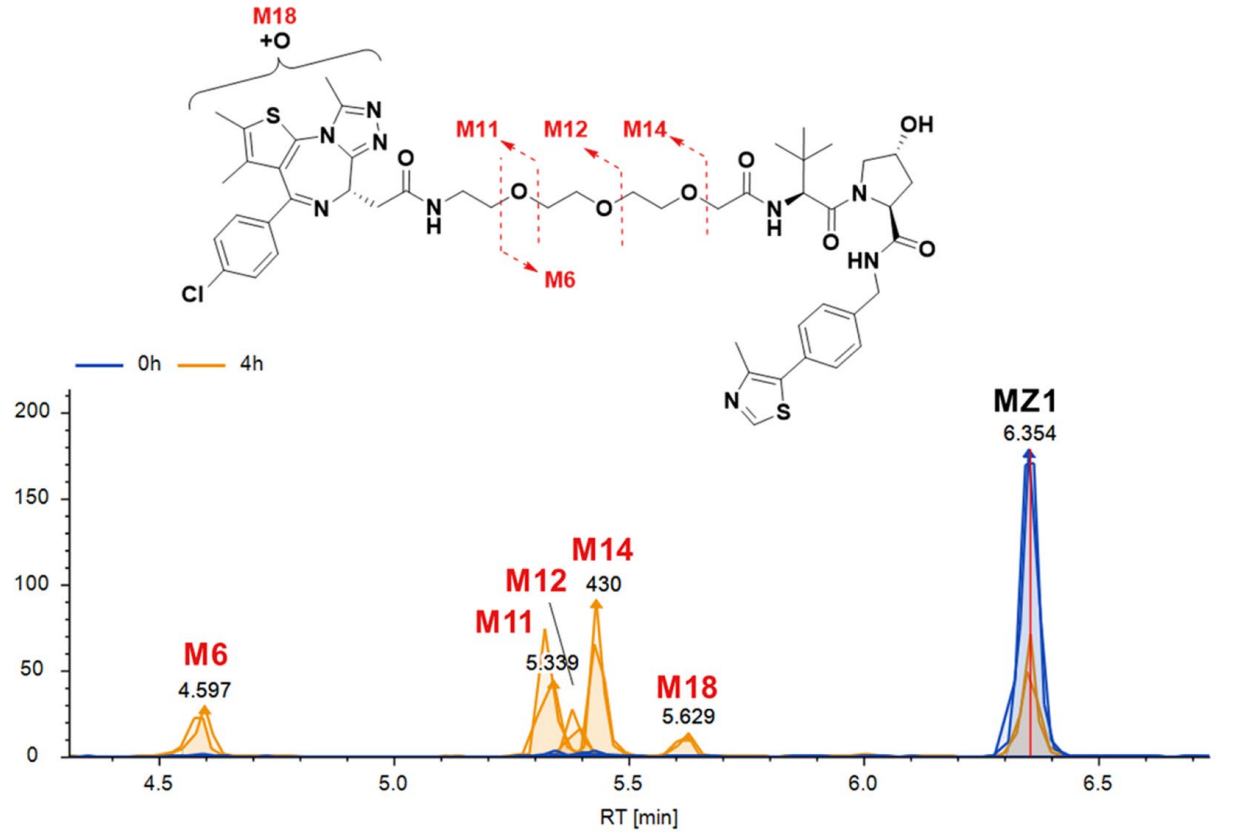

Figure 7. XICs of MZ1 and its five most abundant metabolites, with their transformation sites denoted on the structure above

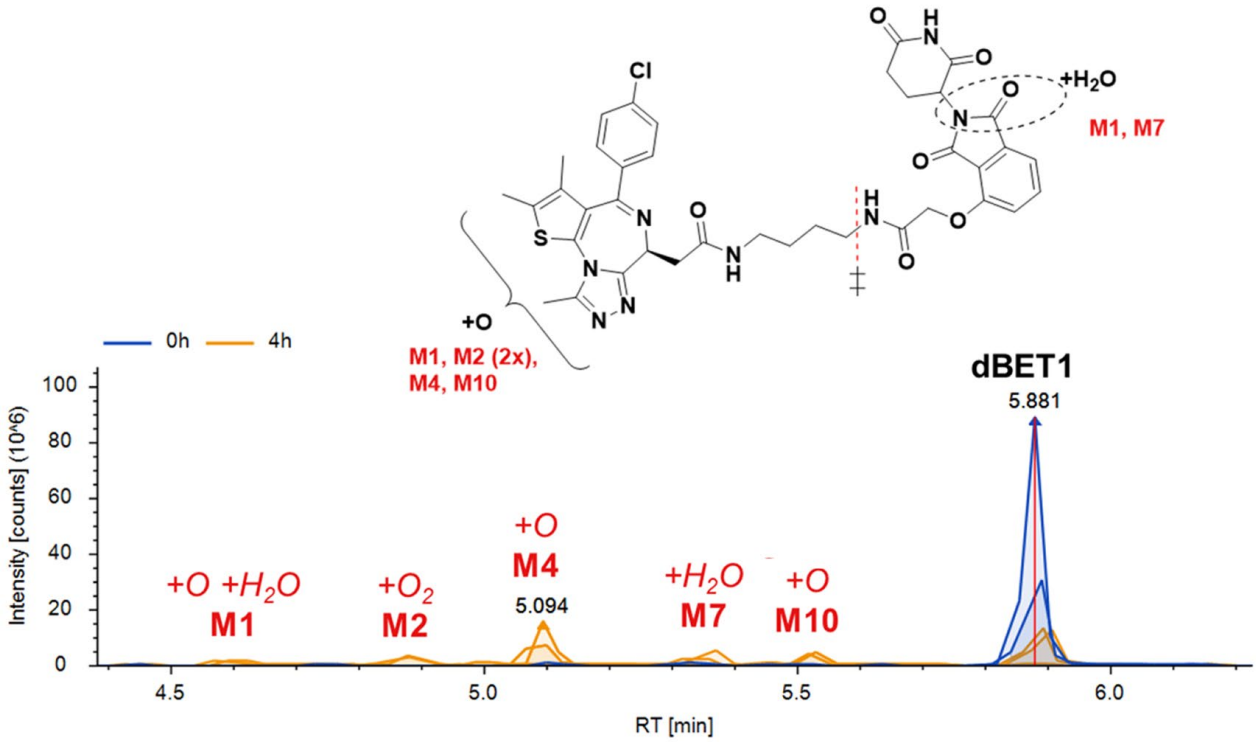

Figure 8. XICs of dBET1 and its five most abundant metabolites, with their transformation sites denoted on the structure above

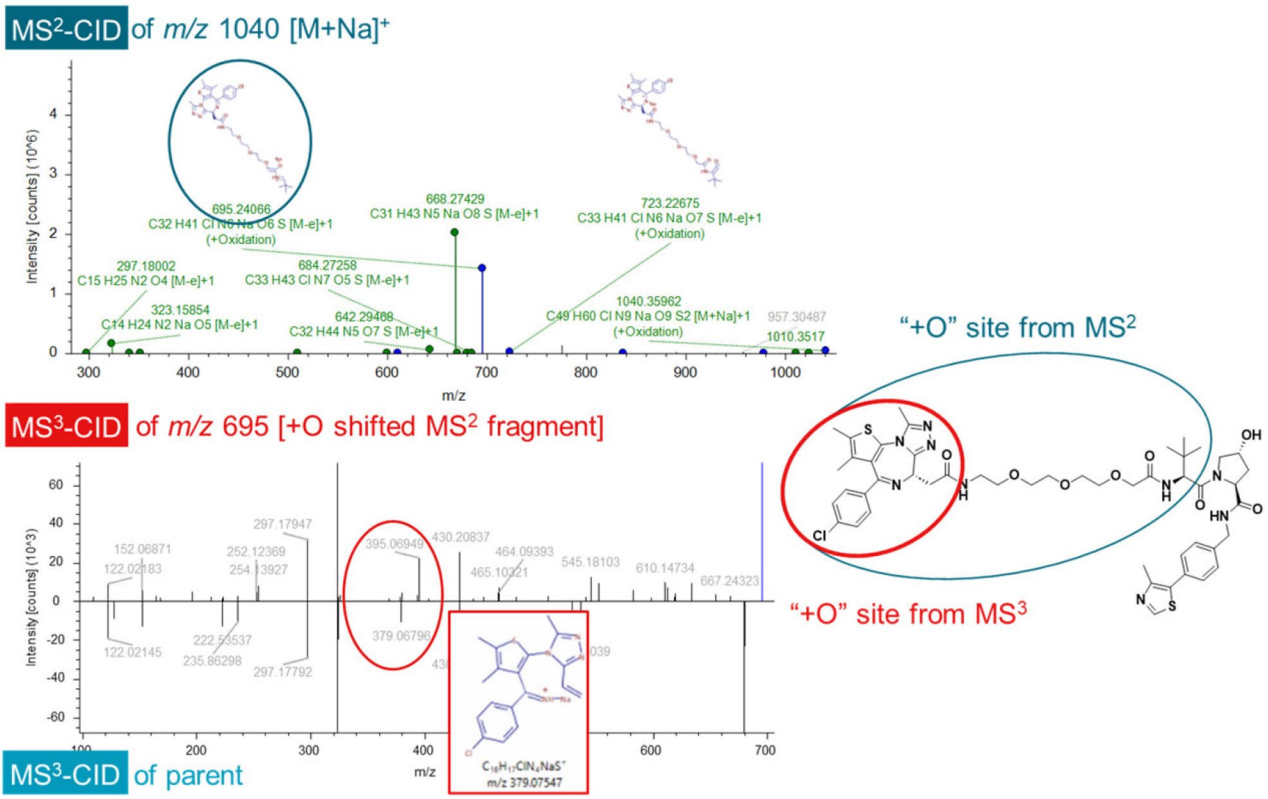

Figure 9. Fragmentation spectra of the [M+Na]+ ion for the oxidized metabolite M18 of MZ1, highlighting the fragment ion assignments allowing the localization of the oxidation site to the BRD4 ligand from the oxidation-shifted MS³ fragment at *m/z* 395

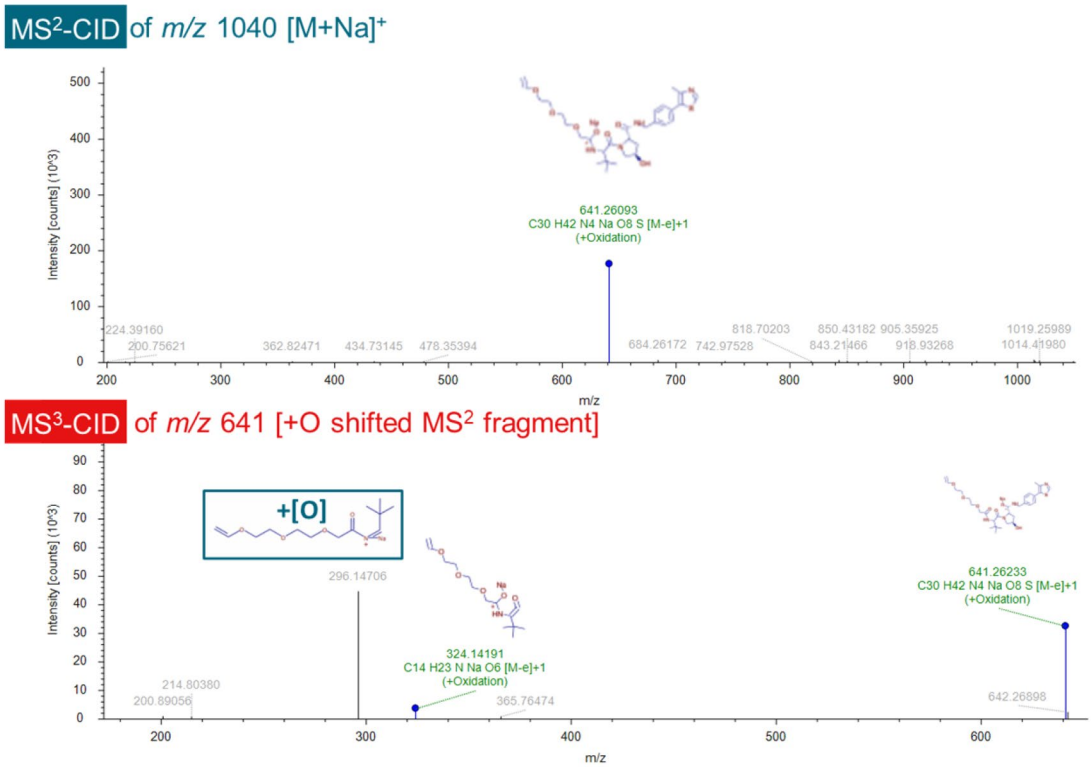

Figure 10. Fragmentation spectra of the [M+Na]+ ion for the oxidized metabolite M23 of MZ1, highlighting the fragment ion assignments allowing the localization of the oxidation site to the linker portion from the oxidation-shifted MS³ fragments

In the metabolism of dBET1, the distinction of regioisomeric metabolites was similarly possible. For instance, two isomeric metabolites corresponding to the hydrolysis ("+H_2O") of dBET1 could be detected at two different retention times (M7 and M8), that could be distinguished based on their MS^2 spectra. In the case of the more abundant M7, the presence of the fragment at *m/z* 675 pointed to the phthalimide as the hydration site, as it could be more readily explained by the loss of the 6-membered glutarimide, which was virtually absent from the MS^2 of M8, as shown in Figure 11.

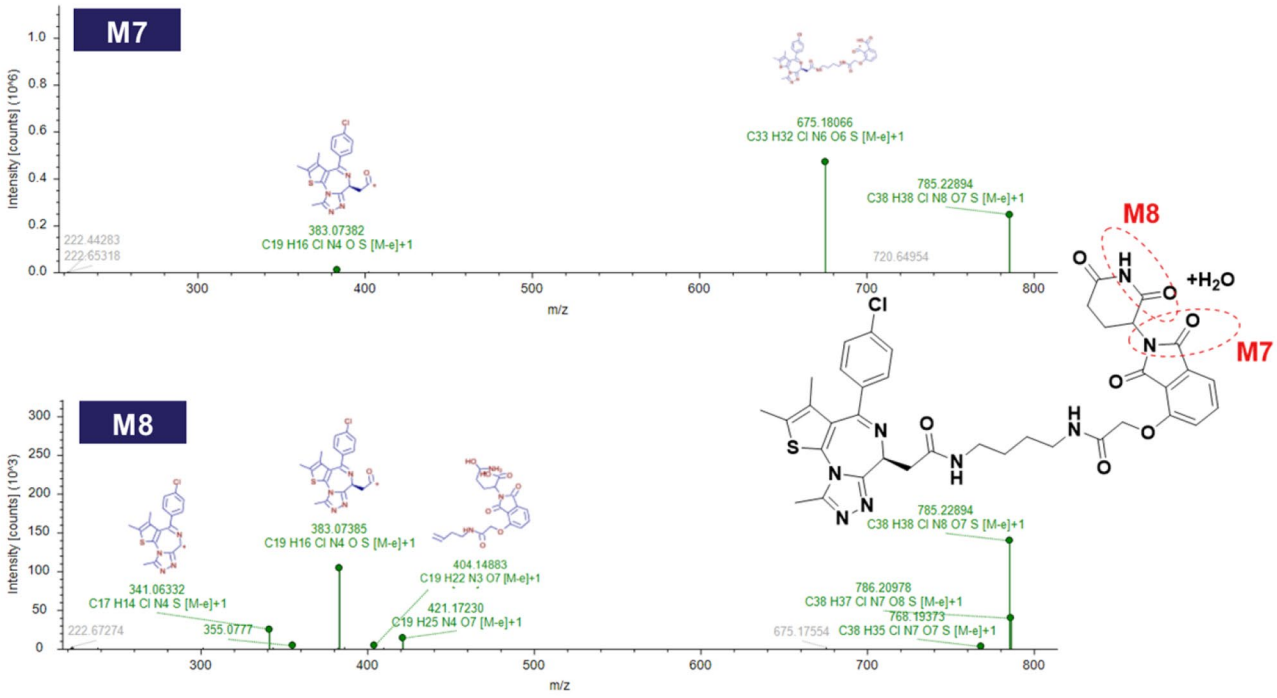

Figure 11. Comparison of the MS^2-CID spectra for the "dBET1+H2O" metabolites M7 and M8 providing evidence for their different ring opening hydrolysis locations

Conclusion

In this work, the *in vitro* metabolism of two model PROTAC compounds could be characterized in depth by utilizing high quality MS^n fragmentation spectra to aid in localization of transformation sites.

- Due in part to their large structures, PROTAC compounds can provide challenges in identifying the site of metabolism.
- The high sensitivity of the Orbitrap Ascend Biopharma Tribrid MS enables structural assignments even from low abundant metabolites with high quality MS^n spectra.
- Automated fragment ion structure annotations in the Compound Discoverer software simplify the structure elucidation of the detected drug metabolites.
- Linker type was found to heavily impact the observed metabolism, with the ethyleneglycol-based linker of MZ1 being a significant contributor to metabolic soft spots in contrast to dBET1.

References

1. Hu, Z. et al. Recent Developments in PROTAC-mediated Protein Degradation: From Bench to Clinic. *Chembiochem* **2022,** *23*, e202100270. doi: 10.1002/cbic.202100270
2. Goracci, L. et al. Understanding the Metabolism of Proteolysis Targeting Chimeras (PROTACs): The Next Step toward Pharmaceutical Applications. *J. Med. Chem.* **2020,** *63,* 11615. doi: 10.1021/acs.jmedchem.0c00793
3. Comstock, K.; Du, M.; Jiang, M. Confident drug metabolite identification using an intelligent data acquisition and processing workflow. Thermo Fisher Scientific Application Note 65953, **2021.** https://assets.thermofisher.com/TFS-Assets/CMD/Application-Notes/an-65953-drug-metabolite-identification-intelligent-data-acquisition-an65953-en.pdf

Appendix

Table A1. Summary of the observed metabolites of MZ1

Name	RT [min]	*m/z*	Reference ion	Calc. MW	Annot. Delta Mass [ppm]	Formula	Dealkylated	Transformations	Composition change	MS Depth	rel.Area 0 hr	rel.Area 4 hr
M1	4.305	505.2115	[M+H]+1	504.2043	0	$C_{24}H_3N_4O_6S$	✓	Oxidation	-($C_{25}H_{28}ClN_5O_2S$)	3	0.2%	0.9%
M2	4.421	489.2167	[M+H]+1	488.2094	0.1	$C_{24}H_{32}N_4O_5S$	✓		-($C_{25}H_{28}ClN_5O_3S$)	2	0.2%	3.5%
M3	4.486	533.2428	[M+H]+1	532.2356	0	$C_{26}H_{36}N_4O_6S$	✓		-($C_{23}H_{24}ClN_5O_2S$)	2	n.d.	0.7%
M4	4.525	548.173	[M+H]+1	547.1657	0.12	$C_{25}H_{30}ClN_5O_5S$	✓	Oxidation	-($C_{24}H_{30}N_4O_3S$)	3	n.d.	1.1%
M5	4.569	591.2483	[M+H]+1	590.2411	0.03	$C_{28}H_{38}N_4O_8S$	✓	Oxidation	-($C_{21}H_{22}ClN_5S$)	2	n.d.	1.3%
M6	4.592	577.2688	[M+H]+1	576.2616	-0.32	$C_{28}H_{40}N_4O_7S$	✓		-($C_{21}H_{20}ClN_5OS$)	2	0.7%	13.9%
M7	5.201	530.1622	[M+H]+1	529.155	-0.18	$C_{25}H_{28}ClN_5O_4S$	✓		-($C_{24}H_{32}N_4O_4S$)	3	n.d.	0.7%
M8	5.216	442.1101	[M+H]+1	441.1029	0.51	$C_{21}H_{20}ClN_5O_2S$	✓		-($C_{28}H_{40}N_4O_6S$)	2	0.6%	0.6%
M9	5.221	570.1543	[M+Na]+1	547.1651	-0.94	$C_{25}H_{30}ClN_5O_5S$	✓	Oxidation	-($C_{24}H_{30}N_4O_3S$)	3	0.5%	0.7%
M10	5.3	530.1625	[M+H]+1	529.1552	0.35	$C_{25}H_{28}ClN_5O_4S$	✓		-($C_{24}H_{32}N_4O_4S$)	3	0.5%	0.5%
M11	5.328	444.1256	[M+H]+1	443.1184	0.22	$C_{21}H_{22}ClN_5O_2S$	✓		-($C_{28}H_{38}N_4O_6S$)	2	1.1%	32.3%
M12	5.387	488.1517	[M+H]+1	487.1445	-0.05	$C_{23}H_{26}ClN_5O_3S$	✓		-($C_{26}H_{34}N_4O_5S$)	2	1.0%	11.2%
M13	5.402	458.1049	[M+H]+1	457.0977	0.24	$C_{21}H_{20}ClN_5O_3S$	✓	Oxidation	-($C_{28}H_{40}N_4O_5S$)	2	n.d.	3.6%
M14	5.431	532.1778	[M+H]+1	531.1705	-0.48	$C_{25}H_{30}ClN_5O_4S$	✓		-($C_{24}H_{30}N_4O_4S$)	3	1.5%	35.1%
M15	5.452	400.0994	[M+H]+1	399.0921	0.07	$C_{19}H_{18}ClN_5OS$	✓		-($C_{30}H_{42}N_4O_7S$)	2	1.0%	1.3%
M16	5.495	546.1571	[M+H]+1	545.1498	-0.39	$C_{25}H_{28}ClN_5O_5S$	✓	Oxidation	-($C_{24}H_{32}N_4O_3S$)	3	n.d.	3.6%
M17	5.507	815.331	[M+H]+1	814.3236	-0.33	$C_{38}H_{51}ClN_8O_8S$	✓		-($C_{11}H_9NS$)	3	n.d.	1.5%
M18	5.625	509.6895	[M+2H]+2	1017.364	-0.03	$C_{49}H_{60}ClN_9O_9S_2$		Oxidation	+(O)	3	0.4%	6.6%
M19	5.822	401.0835	[M+H]+1	400.0762	0.26	$C_{19}H_{17}ClN_4O_2S$	✓		-($C_{30}H_{43}N_5O_6S$)	2	2.6%	3.4%
M20	5.878	1018.371	[M+H]+1	1017.364	-0.51	$C_{49}H_{60}ClN_9O_9S_2$		Oxidation	+(O)	3	0.1%	0.7%
M21	6.012	509.6895	[M+2H]+2	1017.365	0.43	$C_{49}H_{60}ClN_9O_9S_2$		Oxidation	+(O)	3	0.2%	0.8%
M22	6.146	1000.361	[M+H]+1	999.3536	-0.24	$C_{49}H_{58}ClN_9O_8S_2$		Desaturation	-(H_2)	3	0.1%	0.8%
M23	6.153	1018.372	[M+H]+1	1017.363	-1.16	$C_{49}H_{60}ClN_9O_9S_2$		Oxidation	+(O)	1	n.d.	0.4%
M24	6.215	500.6841	[M+2H]+2	999.3535	-0.38	$C_{49}H_{58}ClN_9O_8S_2$		Desaturation	-(H_2)	3	0.1%	1.1%
MZ1	6.355	1002.376	[M+H]+1	1001.369	-0.39	$C_{49}H_{60}ClN_9O_8S_2$				3	100.0%	28.8%

Table A2. Summary of the observed metabolites of dBET1

Name	RT [min]	*m/z*	Reference ion	Calc. MW	Annot. Delta Mass [ppm]	Formula	Composition change	Dealkylated	Transformations	MS Depth	rel.Area: 0 hr	rel.Area: 4 hr
M1	4.592	819.2322	[M+H]+1	818.225	0.12	$C_{38}H_{39}ClN_8O_9S$	$+(H_2O_2)$	✓	Oxidation	3	n.d.	4.3%
M2	4.881	817.2166	[M+H]+1	816.2093	-0.01	$C_{38}H_{37}ClN_8O_9S$	$+(O_2)$		Oxidation x2	3	n.d.	6.6%
M3	4.999	819.2319	[M+H]+1	818.2246	-0.41	$C_{38}H_{39}ClN_8O_9S$	$+(H_2O_2)$	✓	Oxidation	3	n.d.	2.2%
M4	5.094	801.2215	[M+H]+1	800.2142	-0.26	$C_{38}H_{37}ClN_8O_8S$	$+(O)$		Oxidation	3	n.d.	23.2%
M5	5.127	815.201	[M+H]+1	814.1937	0.14	$C_{38}H_{35}ClN_8O_9S$	$-(H_2)+(O_2)$		Desaturation, Oxidation, Oxidation	1	n.d.	1.0%
M6	5.277	799.2057	[M+H]+1	798.1984	-0.37	$C_{38}H_{35}ClN_8O_8S$	$-(H_2)+(O)$		Desaturation, Oxidation	3	n.d.	1.2%
M7	5.351	803.2375	[M+H]+1	802.2303	0.41	$C_{38}H_{39}ClN_8O_8S$	$+(H_2O)$	✓		3	1.5%	9.7%
M8	5.453	803.2378	[M+H]+1	802.2299	-0.12	$C_{38}H_{39}ClN_8O_8S$	$+(H_2O)$	✓		3	n.d.	2.1%
M9	5.484	486.1363	[M+H]+1	485.129	0.25	$C_{23}H_{24}ClN_5O_3S$	$-(C_{15}H_{13}N_3O_4)$	✓	Oxidation	2	n.d.	3.3%
M10	5.525	801.2218	[M+H]+1	800.2145	0.23	$C_{38}H_{37}ClN_8O_8S$	$+(O)$		Oxidation	3	0.7%	7.3%
M11	5.658	801.2215	[M+H]+1	800.2144	0.04	$C_{38}H_{37}ClN_8O_8S$	$+(O)$	✓	*not on that substructure*	3	n.d.	1.3%
M12	5.682	783.2111	[M+H]+1	782.2038	0	$C_{38}H_{35}ClN_8O_7S$	$-(H_2)$		Desaturation	3	0.6%	3.5%
dBET1	5.881	785.2266	[M+H]+1	784.2193	-0.15	$C_{38}H_{37}ClN_8O_7S$				3	100%	26.0%